



**HAL**  
open science

## Simulated annealing effects on Na-FAU crystal reconstruction and sorption efficiency

Panagiotis Krokidas, Eugene D. Skouras, Vladimiros Nikolakis, Vasilis N. Burganos

► **To cite this version:**

Panagiotis Krokidas, Eugene D. Skouras, Vladimiros Nikolakis, Vasilis N. Burganos. Simulated annealing effects on Na-FAU crystal reconstruction and sorption efficiency. *Molecular Simulation*, 2008, 34 (10-15), pp.1299-1309. 10.1080/08927020802208950 . hal-00515039

**HAL Id: hal-00515039**

**<https://hal.science/hal-00515039>**

Submitted on 4 Sep 2010

**HAL** is a multi-disciplinary open access archive for the deposit and dissemination of scientific research documents, whether they are published or not. The documents may come from teaching and research institutions in France or abroad, or from public or private research centers.

L'archive ouverte pluridisciplinaire **HAL**, est destinée au dépôt et à la diffusion de documents scientifiques de niveau recherche, publiés ou non, émanant des établissements d'enseignement et de recherche français ou étrangers, des laboratoires publics ou privés.

## Simulated annealing effects on Na-FAU crystal reconstruction and sorption efficiency

Journal:	<i>Molecular Simulation</i> / <i>Journal of Experimental Nanoscience</i>
Manuscript ID:	GMOS-2008-0051.R1
Journal:	Molecular Simulation
Date Submitted by the Author:	08-Apr-2008
Complete List of Authors:	Krokidas, Panagiotis; University of Patras, Dept. of Materials Science Skouras, Eugene; FORTH, ICE-HT Nicolakis, Vladimiro; FORTH, ICE-HT Burganos, Vasilis; FORTH, ICE-HT
Keywords:	zeolites, reconstruction, sorption

SCHOLARONE™  
Manuscripts

# Simulated annealing effects on Na-FAU crystal reconstruction and sorption efficiency

P. Krokidas<sup>a,b</sup>, E. D. Skouras<sup>a</sup>, V. Nikolakis<sup>a</sup>, and V. N. Burganos<sup>a\*</sup>

<sup>a</sup> Foundation for Research and Technology Hellas, Institute of Chemical Engineering and High Temperature Chemical Processes, Stadiou Str. Platani, P.O. Box 1414, 26504 Patras, Greece

<sup>b</sup> Univ. of Patras, Dept. of Materials Science, 26500, Patras, Greece

## Abstract

The accurate reconstruction of zeolite frameworks at the atomic scale is of critical importance for the study of the sorption and separation properties of these materials. In this work, the atomistic description of NaX FAU crystals is accomplished using lattice reconstruction and simulated annealing techniques. The effect of temperature on the NaX framework structure and on the precise positioning of the extra-framework cations have been thoroughly investigated using annealing cycles at several temperatures. The effects of the framework details including the cation positions on the sorption of CO<sub>2</sub> and N<sub>2</sub> in these structures are studied using molecular simulations. Comparison of simulated adsorption isotherms in non-annealed structures to experimental data reveals that the agreement is a strong function of the cation positions in the framework. More consistent results are obtained when annealing is performed, in which case the deviation in the energy calculations is reduced by almost two orders of magnitude. Cation tracking during several annealing cycles is also implemented that reveals the existence of strongly preferred positions for cations close to the Al atoms within the super cage. Comparison of the calculated and experimental values for the heat of adsorption obtained in this work reveals satisfactory agreement in both CO<sub>2</sub> and N<sub>2</sub> sorption cases for structures that have undergone simulated annealing.

---

\* Corresponding author. E-mail: vbur@iceht.forth.gr

## Introduction

Nowadays, zeolites are involved in an increasingly expanding portion of science and technology, including catalytic and separation processes [1, 2, 3], gas storage [4], and ion exchange [5]. In particular, the performance of a zeolite crystal in separations (sorbents, membranes) can be described by the interplay of the mixture adsorption equilibrium and the mixture diffusion. The prediction of the sorption and separation capacity of a given zeolite membrane should be, in principle, possible on the basis of separately measured single component adsorption and diffusion data. Thus, much experimental and theoretical research effort was focused recently on zeolitic materials. This is driven not only by their technological importance but also by the fact that they provide an inherent representation of model porous systems. Zeolites are well-ordered crystalline nanoporous materials. More than 150 framework types have been identified so far making them ideal systems for the investigation of their adsorption properties against parameters such as size and shape of the pores, chemical composition of the framework (Si/Al ratio, isomorphously substituted Si by other metals, i.e., B, Fe, etc), and nature of the extra-framework cations. In the past few years, a limited number of theoretical studies have investigated the influence of either the nature or the distribution of these cations on the sorption properties of zeolite systems. Systematic studies have focused on the adsorption properties of X- and Y-faujasite systems containing various monovalent or divalent cations [5,6], with respect to different adsorbates, such as carbon dioxide, ammonia, nitrogen, argon, ethane, ethene, and water vapor [7,8]. Such processes are based on specific interactions of the adsorbates with the electrostatic field induced by the cations. These investigations led to empirical relationships showing, for instance, that the heat of adsorption usually increases with increasing charge density of the cations, or with decreasing cation size. It was clearly established that the extra-framework cations play a fundamental role in the adsorption phenomena in such microporous materials.

The modeling process of the separation behavior of a zeolite membrane is still at early stages of development. Recently, the Maxwell-Stefan model has been successfully employed for the description of the single component permeation [9] and the prediction of binary mixture permeation [10] in MFI membranes. Two transport

1  
2  
3  
4 mechanisms are assumed to overlap: surface diffusion and activated gas diffusion.  
5  
6 Based on Molecular Dynamics and Molecular Orbital calculations it has been  
7  
8 attempted to describe and forecast molecular permeation by computer simulation. A  
9  
10 more detailed classification of the two-component permeation through zeolitic  
11  
12 membranes considers (i) adsorption on the external surface, (ii) selective adsorption in  
13  
14 the zeolite pores and (iii) size dependent diffusivities in the zeolite pores.

15  
16 Zeolite membranes can separate a mixture via a molecular sieving process or due to  
17  
18 large differences between the individual molecular mobilities, large differences  
19  
20 between the adsorption potentials for each compound, or a combination of mobility  
21  
22 and adsorption potential differences. In the case of differences in adsorption, the  
23  
24 selectively adsorbed compound excludes the other one from entering the zeolite pores,  
25  
26 and as a result it blocks its transmission through the membrane.

27  
28 In the past, atomistic simulations of the structure of several inorganic porous materials  
29  
30 (SiO<sub>2</sub>, zeolites) [11-17] have been realized using Molecular Dynamics and Monte  
31  
32 Carlo simulations. The reconstruction of inorganic structures at the atomic scale  
33  
34 usually includes the following conceptual steps. Initially, the atoms of the membrane  
35  
36 material are positioned at reference bulk lattice sites using literature data. The  
37  
38 interatomic potential energy of the configuration is dynamically calculated using a  
39  
40 pre-selected force field description, the parameters of which have been calculated  
41  
42 using either experimental or *ab-initio* data. Depending on the available data and the  
43  
44 accuracy needed, simple energy descriptions, like the ones found in Universal Force  
45  
46 Field (UFF) [18] (as well as in UFF variations), adapted to zeolite simulations [19,20]  
47  
48 can be utilized for this purpose [21,22]. Boundary conditions are then set, either  
49  
50 periodic or of the free surface type. The final step is the total potential energy  
51  
52 minimization of the system, using Steepest Descent, Conjugate Gradient and Newton-  
53  
54 Raphson techniques, and addition of cation or other bulk/surface defects (where  
55  
56 appropriate) in an iterative scheme. Using a force field of this kind, very useful  
57  
58 quantities can be computed, such as momenta, interaction energies, conformational  
59  
60 energy barriers, free energies, etc. The atomistic structure is the basis for MD and MC  
calculations to probe the locations, conformations, and motions of sorbate molecules,  
such as CO<sub>2</sub>, and N<sub>2</sub>, in order to draw useful conclusions concerning the actual supply  
of sorbates to the active sites of various types of FAU structures (DAY and NaX).

1  
2  
3  
4  
5  
6  
7  
8  
9  
10  
11  
12  
13  
14  
15  
16  
17  
18  
19  
20  
21  
22  
23  
24  
25  
26  
27  
28  
29  
30  
31  
32  
33  
34  
35  
36  
37  
38  
39  
40  
41  
42  
43  
44  
45  
46  
47  
48  
49  
50  
51  
52  
53  
54  
55  
56  
57  
58  
59  
60

In the present work the adsorption of CO<sub>2</sub> and N<sub>2</sub> in atomistic reconstructions of the Na-form of the aluminosilicate faujasite (FAU) is studied. The interest in the particular zeolite stems from promising experimental data on their separation efficiency in the form of polycrystalline membranes [23,24]. This goal is achieved through the following procedure: An initial structure of the FAU crystal is reconstructed at the atomic level using data from the literature. However, the existing data are usually available only at room temperature, and they do not provide information about the exact position of the extra-framework cations that are present in the structure. To address these issues, a general methodology using simulated annealing is developed and used for the atomistic description of NaX FAU crystals. Adsorption isotherms are then calculated and compared with experimental results, and along with heats of adsorption, they are used for the validation of the simulation methodology proposed here. Simulated annealing is found to lower significantly the uncertainties in the prediction of sorption and separation properties of FAU.

### Computational methodology

The faujasite unit cell having a stoichiometry close to that of experimentally investigated samples has been reconstructed using the XRD-based structural data from the work of Zhu and Seff [25]. The unit cell of NaX has cubic symmetry (Fd3m symmetry group) and its lattice constant at room temperature is 25.077 Å. The composition of the unit cell is O<sub>384</sub>Si<sub>100</sub>Al<sub>92</sub>Na<sub>92</sub>. Previous studies, like the one of Buttefey *et al* [26], assumed that both Si and Al can be represented using a unique T atom that had the average properties of the two atoms. This assumption was introduced to sidestep the complication that would arise by the large number of possible configurations of the same crystal if Si/Al is not equal to one. If a unique T atom is not introduced, then a reliable computation of a property would require a large number of simulations in order to average over the different arrangements of Al atoms in the simulated unit cell. This number can be extremely high in the case of zeolites with high Si/Al ratio (case of NaY). On the other hand, Jaramillo and Auerbach have developed a forcefield for modeling cation motion in faujasite that explicitly distinguishes between the Si and Al atoms [27]. The minimum energy configuration

of several faujasite crystals having different Si/Al ratio was obtained using a cation annealing procedure. The T-atom methodology was not used in the present work, for two reasons. First, we studied a NaX crystal of the aforementioned composition (Si/Al =1.16), in which only four Al framework atoms have to be arranged (four degrees of freedom), thus keeping the uncertainty of the resultant configuration rather limited. Second, given that one of the goals of this study was to simulate the adsorption in NaX crystals, the clear distinction between Si and Al atoms is needed to provide a detailed simulation of the sorption process. Thus, the first step in the reconstruction is the proper placement of the Si, Al and O framework atoms, which form eight sodalite cages in FAU. Sodalite cages are interconnected with oxygen bridges forming a pore system with access window having diameter *ca.* 7.4 Å. The Si and Al atom distribution follows the Löwenstein's Al-O-Al avoidance rule [28]. The placement of the cations at specific sites is very significant also [29,30]. A view of the reconstructed unit cell of NaX, obtained with the help of Materials Studio, is shown in Figure 1, where the red balls represent the oxygen atoms, whereas the purple and yellow balls represent the aluminum and silicon atoms, respectively. The blue balls represent the Na cations.

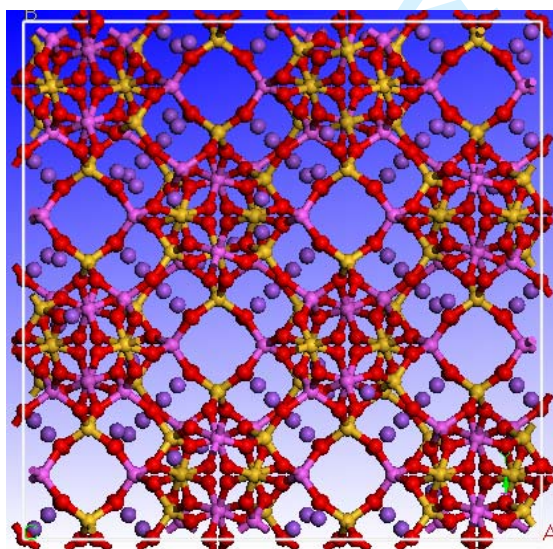


FIGURE 1. Unit cell of NaX faujasite.

The possible positions of  $\text{Na}^+$  in the unit cell are the following: sites I located in the center of the double six member ring connecting the sodalite cages; sites I' located in the sodalite cage in front of the double six member ring; sites II in front of the single

6-ring window of sodalite cage; and sites III' and III'', which are congener positions located in front of the 4-ring windows of the sodalite cages with small variations and called here sites III. Figure 2 shows a schematic representation of the Na<sup>+</sup> positions in the various sites, using as point of reference a sodalite cage.

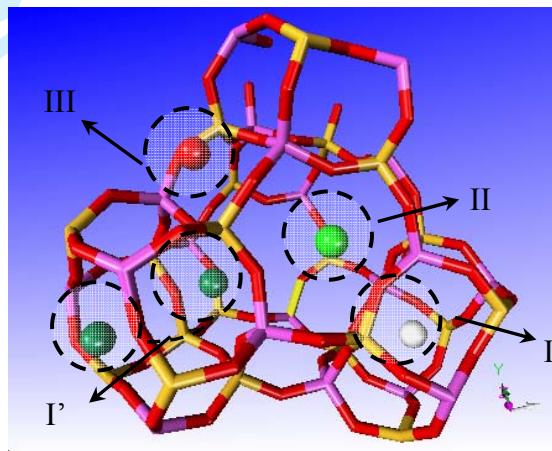


FIGURE 2. The possible locations of Na<sup>+</sup> in faujasite using the sodalite cage as a point of a reference.

The distribution of Na<sup>+</sup> among the different sites involved 32 Na<sup>+</sup> at sites I', 32 Na<sup>+</sup> at sites II, and 28 Na<sup>+</sup> at sites III. In the case of NaX, full occupancy of sites I' and II was assumed (32 Na<sup>+</sup>/site). This is not the case for sites III, where only 28 of the 196 symmetrical positions are occupied. This means that several alternative configurations with the Na<sup>+</sup> at different locations can be generated. Two possible methods were followed in order to reproduce an energy favoring structure. The first method is the one suggested in the work of Seff [25], and the second one places the Na<sup>+</sup> cations randomly, excluding positions that are too close to each other and, consequently, would produce unrealistic, repulsive interactions.



### Interaction potential

We separate the forces that act on the zeolite atoms in the presence of gas molecules into intermolecular and intramolecular ones. The intermolecular (non-bonded) interaction energy,  $V_n$ , is due to interactions among atoms of different molecules. Interactions between atoms of the same molecule or between bonded atoms are called intramolecular interactions (bonded) and correspond to the interaction energy  $V_b$ . The overall interaction energy is the sum of these two contributions:

$$V = V_b + V_n \quad (1)$$

### Intermolecular interactions

Intermolecular interactions are described with a Lennard – Jones potential for the Van der Waals interactions and a term for the electrostatic interactions. The general form of the relation giving the intermolecular interactions is given below:

$$V_n = V_{L-J} + V_{electrost} \quad \text{where} \quad \left\{ \begin{array}{l} V_{L-J} = 4\epsilon \left[ \left( \frac{\sigma}{r} \right)^{12} - \left( \frac{\sigma}{r} \right)^6 \right] \\ V_{electrost} = \underbrace{\frac{q_1 q_2}{4\pi\epsilon r}}_{\text{Charge-charge}} - \underbrace{\frac{\mu q}{4\pi\epsilon}}_{\text{Charge-dipole}} \otimes \underbrace{\frac{1}{r^2}}_{\text{Dipole-dipole, charge-quadrupole, etc.,..}} + .. \end{array} \right. \quad (2)$$

The interaction of the gas molecules ( $\text{CO}_2$  and  $\text{N}_2$ ) with each other and with the zeolite atoms has been described using the point charge model. In this approach every atom interacts independently of the others, and a specific charge is assigned to every atom in each gas in order to reproduce the quadruples of  $\text{CO}_2$  and  $\text{N}_2$ . Figure 3 shows quadruples of  $\text{CO}_2$  and  $\text{N}_2$ . An alternative approach is the united atom method, where every molecule is represented as an interaction center, assigned a Van der Waals term and a term giving its electrostatic moment. Clearly, the former model gives a detailed and, thus, more realistic description of the way the molecules interact with each other and with the lattice atoms, provided that sufficient forcefield data for each interaction are available, which is the present case. The form of the relation for the interactions

now looks simpler, since the charges of the atoms are only needed for the description of the electrostatic interactions:

$$V_n = 4\epsilon \left[ \left( \frac{\sigma}{r} \right)^{12} - \left( \frac{\sigma}{r} \right)^6 \right] + \frac{q_1 q_2}{4\pi\epsilon r} \quad (3)$$

The molecules studied here are linear quadruples, so they were represented as three-point models, i.e. three points on the same line, the central atom having a specific charge and the outer ones having half the charge of the central one. Figure 3 shows the quadruples for the CO<sub>2</sub> and N<sub>2</sub> molecule. In the case of N<sub>2</sub>, which is a diatomic molecule, the central point is a pseudoatom which does not interact via the Van der Waals force. It serves only as a position with a specific charge that is generated in the center of the bond between the two atoms and is responsible for the quadruple character of the molecule.

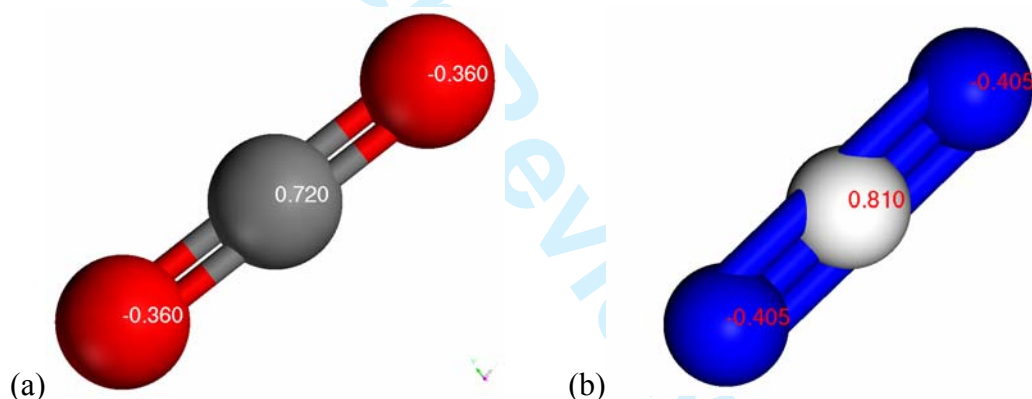


FIGURE 3. Representation of quadruple molecules of (a) CO<sub>2</sub> and (b) N<sub>2</sub>.

The values for the charges and the distances between the point charges forming the quadruples as well as the values for the terms of the Lennard–Jones potential used in the simulations can be found in Tables I and II, respectively. The CO<sub>2</sub> charges were derived with the use of *ab initio* calculations, while the Lennard–Jones parameters were obtained by fitting with experimental adsorption enthalpies [31]. The charges and the diagonal Lennard–Jones parameters for the N<sub>2</sub> molecule are the product of a fitting procedure using experimental data of properties of the crystal structure of nitrogen at zero temperature [32]. Further details for the structure charges and potential parameters can be found in the literature [33], [34].

**Table I.** Charges and interatomic distances used in the simulations

Atom	Charge	Interatomic distance (gas molecules) / Å
Si (framework)	2.4	
Al (framework)	1.7	
O (framework)	-1.2	
C (in CO <sub>2</sub> )	0.72	
O (in CO <sub>2</sub> )	-0.36	1.150 (C–O)
N (in N <sub>2</sub> )	-0.483	1.098 (N–pseudo atom)
pseudo-atom #1 (in N <sub>2</sub> )	0.966	

The electrostatic interactions were calculated using the Ewald summation method, and the Van der Waals terms were calculated from an atom-based summation with 12 Å cut-off distance.

**Table II.** Van der Waals constants for the interaction of N<sub>2</sub> with the framework atoms and within the CO<sub>2</sub> molecule

N <sub>2</sub> [32]	N	O <sub>z</sub>	Na <sup>+</sup>				
$\epsilon_N$ (eV)	0.00314	0.0197	0.00434				
$\sigma_N$ (Å)	3.318	2.708	1.746				
CO <sub>2</sub> [31]	O-O	C-C	O-C	C-O <sub>z</sub>	O-O <sub>z</sub>	C-Na	O-Na
$\epsilon_N$ (eV)	0.00659	0.00402	0.00158	0.00363	0.00601	0.00759	0.0027
$\sigma_N$ (Å)	3.36	3.83	3.31	3.90	3.48	3.35	2.95

### *Intramolecular/bond interactions*

The motion of the Na cations in faujasite has been modeled in the past. However, in the previous studies [26,35] the movement of the framework atoms was usually ignored. Our goal was to develop a technique that can predict at different temperatures not only the cation arrangement but also the exact framework atom positioning. For this reason, a full potential model, containing interactions between both framework atoms and cation atoms was adopted.

Bonded terms in the potential expression adopted stand for forces that are generated between bonded atoms and describe the pertinent atomic motions, like oscillations and vibrations of the atoms around the equilibrium positions. These movements were used in the annealing process, where the motion of the framework as well as the vibrations of the gas molecules must be taken into account.

A theta harmonic potential was used, which describes the oscillations of the angle of the bond between Al and O atoms as well as between Si and O atoms. The theta harmonic potential has the form:

$$E = 1/2K_{\theta}(\theta - \theta_0)^2 \quad (4)$$

The Buckingham potential provides updated Van der Waals force terms for zeolitic atoms. The Buckingham potential is of the form

$$V(r) = A \exp(-r / \rho) - Cr^{-6} \quad (5)$$

where  $\rho$  is a characteristic distance between the atoms (see below). While the aforementioned equation is the most commonly used, a different yet equivalent form of it was used in our calculations (Materials Studio; FORCITE, Soprtion modules):

$$V(r) = D_0 \left[ \left( \frac{6}{\gamma - 6} \right) \exp \left( \gamma \left( 1 - \frac{r}{R_0} \right) \right) - \left( \frac{\gamma}{\gamma - 6} \right) \left( \frac{R_0}{r} \right)^6 \right] \quad (6)$$

We found the equivalent parameters for the Materials Studio description by matching the field values description of equations (5) & (6) and solving the corresponding algebraic system (7),

$$D_0 \left( \frac{6}{\gamma - 6} \right) \exp(\gamma) = A$$

$$\frac{\gamma}{R_0} = \frac{1}{\rho} \quad (7)$$

$$D_0 \left( \frac{\gamma}{\gamma - 6} \right) R_0^6 = C$$

where  $D_0$  is the bond strength or well depth of the potential in kcal/mol,  $R_0$  is the bond length in Å, and  $\gamma$  is a scaling factor. The Buckingham potential does not represent a bonded potential but can be used for describing interactions between atoms belonging to a single body (zeolite).

The parameter values for these detailed potentials have been taken from the literature [20]. Coarser descriptions, like the Rigid Unit Model (RUM) [35], which provide interactions between rigid groups of atoms (tetrahedra and octahedra) linked by vibrating oxygen bridges, have been used in the past for the investigation of the zeolite structure deformation, like temperature dependence of the zeolite pore dimension, and negative thermal expansion coefficients.

Absolute adsorption isotherms were computed using a Grand Canonical Monte Carlo calculation algorithm, which allows displacements (translations and rotations), creation, and destruction, as implemented in the Sorption module of the Materials Studio software suite. These simulations consisted in evaluating the average number of adsorbate molecules whose chemical potential equals that of the bulk phase for a given fugacity (pressure) and temperature. In order to compare simulations with experimental data, the fugacity ( $f$ ) and pressure ( $p$ ) were related through  $f = cp$ , where  $c$  corresponds to the fugacity coefficient. This coefficient is known to vary with pressure and in the present work it was evaluated through an experimentally derived equation of state that accounts for gas compressibility. In fact, the gas compressibility was calculated with the aid of tables that correlate this quantity with the critical pressure and critical temperature of each sorbate. Further information on the relation among these quantities and on the origin and content of the aforementioned tables can be found in the literature [36].

All simulations were performed at 293-333 K using one unit cell of faujasite, typically allowing  $3 \times 10^6$  to  $5 \times 10^6$  Metropolis Monte Carlo (MC) steps (for further information

about the MC algorithm, the reader is referred to the related textbook of Frenkel and Smit [37]). The evolution of the total energy over the MC steps was plotted in order to control the equilibrium conditions. The zeolite structure was assumed to be rigid during the sorption process. This is a convenient yet rather reasonable assumption for the sorption process, as the heat of adsorption is primarily a function of the sorbate-framework interactions, provided that the framework is near equilibrium. However, during minimization and simulated annealing, this assumption is removed thanks to the large flexibility in the degrees of freedom that is allowed in these cases. Cell angles and bond lengths were kept rigid at their minimum-energy locations as pinpointed by the forcefield description.

The Ewald summation was used for the calculation of the electrostatic interactions, while the short-range interactions were calculated using a cutoff distance of 12 Å. Furthermore, in order to take into consideration the steric effects that prohibit the access of N<sub>2</sub> and CO<sub>2</sub> atoms into the sodalite cages, dummy atoms with appropriate van der Waals radii were mounted into these cages. As a result, the selection of a location in the sodalite cages as an adsorption site by the MC algorithm became practically impossible. The calculations of the differential enthalpies of adsorption at zero coverage,  $\Delta_{\text{ads}}h_{\theta}$ , can be performed through the fluctuations of the number of particles in the system and through the fluctuations of the internal energy  $U$ , (i) with the consideration of very low pressures and (ii) by switching off the adsorbate-adsorbate interactions.

$$\Delta_{\text{ads}}h = RT - \frac{\langle U \cdot N \rangle - \langle U \rangle \langle N \rangle}{\langle N^2 \rangle - \langle \langle N \rangle \rangle^2} \quad (8)$$

### *Simulated annealing*

The annealing process consists of simulation steps that include two main parts, the first of which employs conjugate gradient techniques for the energy minimization of the structure at hand using a forcefield description of the interactions between atoms [38]. This part is followed by a NVT molecular dynamics part. At sequential steps, the temperature value is gradually increased from the initial one up to a predefined temperature limit (increasing ramp). This procedure is followed by a similar one, with gradually lower MD temperatures (decreasing ramp), down to the initial temperature.

This increasing-decreasing ramp cycle is usually followed by several sequential ones to optimize results. The idea behind the simulated annealing technique is to use the MD steps and the temperature ramp to overcome local energy minima of the structure and, thus, achieve a structure configuration with a total energy minimum [38]. This would not be possible if a simple minimization technique was used.

## Results and Discussion

As the starting point of the annealing process, the most appropriate set of numerical parameter values, including those of the number of cycles, ramps, and dynamic steps, was investigated. Initial attempts were conducted with 5 cycles and 5 ramps per annealing cycle, and the structure was allowed to move for 40000 dynamic steps (of 1 fs) within each ramp, leading to a total of  $10^6$  steps. The numbers of steps and ramps were kept fixed within a simulation, the maximum temperature was set at 533K and the initial (target) temperature was 293K. This temperature corresponds to room conditions and is quite close to the one at which literature X-ray data were taken and used for the reconstruction of the initial structure [25]. Table III summarizes the results of this procedure. For 5000 dynamic steps, a structure of similar energy was generated. The number of dynamic steps was gradually reduced to a number that can reproduce the equilibrium velocity distribution in the NVT ensemble at the desired temperature. A number of 50 to 100 dynamic steps turned out to be sufficient for the system to reach equilibrium. Thus, a number of 50 dynamic steps per ramp were used, while the number of cycles was set at 15 and the number of ramps at 10, thereby lowering the total steps to 7500. Using these optimal parameters, a crystal of the same level of energy, and of practically the same volume, was obtained, saving valuable computational time.

**Table III.** Parameters and results (final volume and energy of structure) for each annealing process.

	<i>Cycles</i>	$T_{max}$	<i>Ramps</i>	<i>Dynam. Steps/ Ramp</i>	<i>Volume (<math>\text{\AA}^3</math>)</i>	<i>Energy (<math>\text{kcal/mol} \cdot 10^{-5}</math>)</i>

Initial	-	-	-	-	15769.8	-1.98075
1	5	533	5	40000	15142.2	-2.011194
2	5	533	5	10000	151498	-2.011126
3	5	533	5	5000	15141.35	-2.011158
4	15	533	10	50	15143.22	-2.011199

For validation purposes, an investigation was performed, in order to seek whether the results could indeed converge to the same structure (of minimum total energy), independently of the precise selection of the initial structure configuration. To this end, several different structures were reconstructed, using data from the work of Seff [25]. The initial structures were divided into two groups. The first one involved unit cells in which the Na<sup>+</sup> cations at sites III' and III'' were distributed using the procedure reported in [25]. In the second group, the III'/III'' site cations of the unit cell were distributed following a fully random process. The results are shown in Table IV. The number of steps that was ultimately chosen (7500) was the one which could reproduce energetically acceptable cells in the minimum simulation time without compromising noticeably the accuracy (in both geometric and energy terms) of the results. Once again, the target temperature was set at 293K. All unit cells had an initial volume of 15769.8 Å<sup>3</sup>. The different distributions of Na<sup>+</sup> led to an energy deviation between the structures of ca 340kcal/mol. On the other hand, the simulated annealing procedure, as performed on these structures, resulted in structures of lower volume by about 4%, as compared to the initial structures, and limited drastically the energy deviation down to ca 8 kcal/mol despite the large deviations that were noted among the initial structures.

**Table IV.** Energy and structure deviations of the various reconstructed cases (before and after simulated annealing)

	<i>Initial Volume</i>	<i>Initial Energy</i>	<i>Energy Deviation</i>	<i>Final Volume</i>	<i>Final Energy (kcal/mol)</i>	<i>Energy Deviation</i>



	( $\text{\AA}^3$ )	(kcal/mol)	(kcal/mol)	( $\text{\AA}^3$ )	(kcal/mol)	
Random 1	15769.8	-198074.52	339.421	15143.22	-201120	7.855
Random 2		-197959.24		15136.45	-201103	
Random 3		-198007.68		15139.94	-201100	
Seff 1		-198638.10		15141.53	-201102	
Seff 2		-198619.64		15140.49	-201106	

The new positions of  $\text{Na}^+$  at III'/III'' sites were also checked through radial distribution functions. Indeed, while Na III' remained close to Al atoms, Na III'' atoms moved away from Si atoms and repositioned themselves in the vicinity of Al atoms. This appears to be a naturally preferable position for  $\text{Na}^+$ , since Al atoms are assigned smaller positive charge. In general, during the annealing process the only considerable transfer took place between  $\text{Na}^+$  of III' and III'' sites, while  $\text{Na}^+$  at I' and II sites remained close to their initial positions. This behavior was also evident in the radial distribution function of NaX structures that were annealed subsequently at elevated temperatures, as described in the following section.

In order to validate further the proposed modeling methodology, the sorption capacity of the reconstructing crystals was calculated and compared to experimental data both at room temperature and at higher temperatures. The simulated annealing process was expanded to higher temperatures up to 325 K. Table V shows the main features of the annealed unit cells at four different temperatures. The structure at each temperature was used as initial geometry in order to generate a structure at the next temperature in sequence. The reason is that it is preferable to use as initial guess a structure that corresponds to the closest possible temperature to the desirable one. Theoretically, it would be ideal to be able to allow infinitesimally small temperature steps but this would be extremely time consuming.

**Table V.** Variation of the cell volume and the potential energy on the simulated annealing temperature

<i>Annealing Temp.</i> (K)	<i>Cell Volume</i> (Å <sup>3</sup> )	<i>Energy</i> (kcal/mol)
293	15142.09	-200440
302	15143.32	-201081
311	15142.42	-201114
325	15140.59	-201099

The significant decrease of the minimum energy uncertainty that is offered by the simulated annealing procedure renders the method very attractive for further applications, including adsorption and diffusion. However, care must be taken to allow sufficient time for equilibration at the different intermediate stages to ensure not only energy minimization but also settling of the Na III' and Na III'' atoms at their equilibrium positions. This can be done by studying the radial distribution of the Na III' and Na III'' positions next to the Al and Si atoms. Figure 4 shows the Na<sup>+</sup> positions after annealing procedure at different temperatures. White-filled bars show Na cations that are initially next to Si atoms (sites III'') and black-colored show the ones that are initially next to Al atoms (sites III'). It appears that the positions next to the Al atoms (III') are most preferred by the Na cations thanks to their weaker electrostatic repulsion by the Al atoms compared to that by the Si atoms. Jaramillo and Auerbach [27] have also predicted two distinct cation positions in the Na<sub>86</sub>X and the Na<sub>96</sub>X faujasites. However, our work reveals that at elevated annealing stages, a number of cation positions equidistant to Si and Al atoms (sites III, hatches) are increasingly occupied by Na atoms. The existence of such sites has also been reported by Olson [39] who determined the faujasite structure from X-ray diffraction data. Thus, the simulated annealing technique facilitated the overcome of energy barriers during minimization. In fact, it is expected that the precise positioning of the Na cations will affect eventual gas loading, as will be discussed below. At this point we have to stress the fact that the proposed methodology provides a clear distinction between three particular positions belonging to the III site family, while Buttefey *et al*

[26] only mention two. This differentiation is originated from the fact that Buttefey *et al* used a single atom (T) to describe both Al and Si atom 4444positions and, thus, a differentiation between III' and III" positions was not feasible.

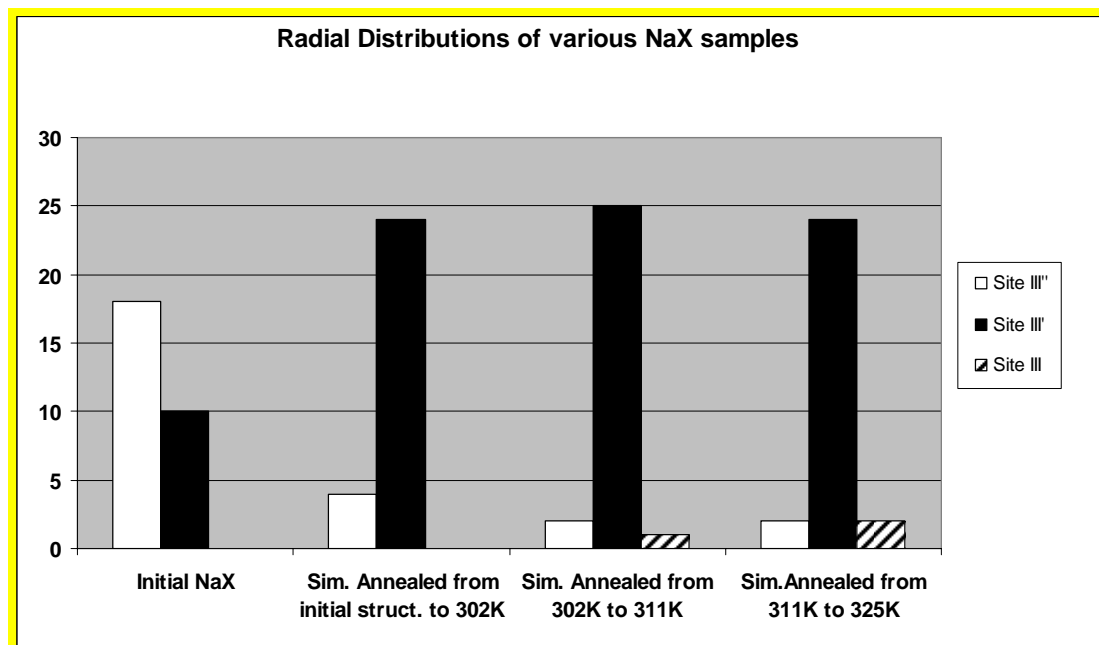


FIGURE 4. Occupation of sites III', III'' and III with Na atoms positioned nearby Si and Al framework atoms (taken from radial distribution functions) in various NaX samples at 302K: Initial NaX structure (non-annealed); NaX structure annealed at 302K (starting from the initial structure); NaX structure annealed up to 311K (starting from the 302K-annealed structure); and NaX structure annealed to 325K (starting from the 311K-annealed structure).

### Sorption results

The sorption of CO<sub>2</sub> and N<sub>2</sub> molecules was simulated at different temperatures in the initial unit cell, as well as following annealing at several temperatures. The synthesis of NaX crystals and the experimental procedure for measuring the adsorption isotherms for CO<sub>2</sub> and N<sub>2</sub> has been described in previous publications [40-43]. Calculated adsorption isotherms were compared with experimental ones. Figure 5 shows that the adsorption isotherms for non-annealed reconstructed unit cells compare satisfactorily with the experimental ones that were obtained in this work but exhibit

1  
2  
3  
4  
5  
6  
7  
8  
9  
10  
11  
12  
13  
14  
15  
16  
17  
18  
19  
20  
21  
22  
23  
24  
25  
26  
27  
28  
29  
30  
31  
32  
33  
34  
35  
36  
37  
38  
39  
40  
41  
42  
43  
44  
45  
46  
47  
48  
49  
50  
51  
52  
53  
54  
55  
56  
57  
58  
59  
60

large variations among each other especially at the elevated temperature (325 K). In fact, a small deviation between experimental and theoretical isotherms is inevitable mainly due to the large number of choices between possible cation positions (occupancies) but also due to the structural differences that are expected between the temperature of the XRD refinement and the temperature used in the calculations. Among the objectives of the annealing method is to reconstruct framework geometries that will reproduce experimental data (adsorption isotherms) with limited deviation among realizations. In this work, annealing turns out to be very efficient in reproducing satisfactory structures that lead to adsorption isotherms with notably smaller deviations, compared to those of the isotherms of structures prior to annealing. However, the deviation from experimental data increases at increased temperature. Nevertheless, this deviation is clearly smaller than the typical deviation among different sets of experimental data for the same process and the same temperature, as shown by a literature survey [44,45,46]. Structure annealing appears to improve the estimation of the heat of adsorption (Figure 6). A Langmuir fit to the relevant experimental data for sorption rendered a value of 6.8 kcal/mol, while the calculated values for heat of CO<sub>2</sub> sorption for non-annealed and annealed structures were 10.7 and 8.7 kcal/mol, respectively.

In the case of N<sub>2</sub> sorption, the annealed structures provided adsorption isotherms (Figure 7) that are in very good agreement with the experimental ones and at the same time with much smaller deviation compared to that of non-annealed structures. The heat of adsorption (Figure 8) is also predicted with satisfactory accuracy considering again all factors that may have introduced some ambiguity in the precise reconstruction of the framework, as discussed above.

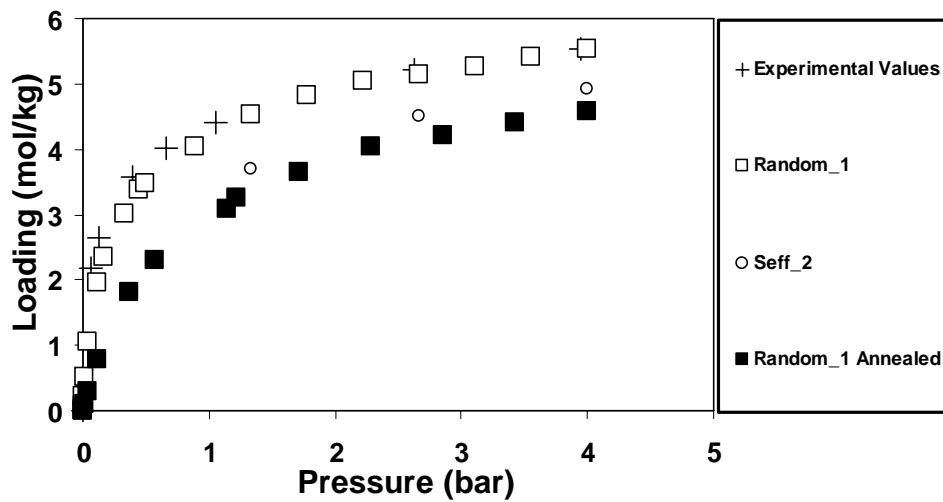
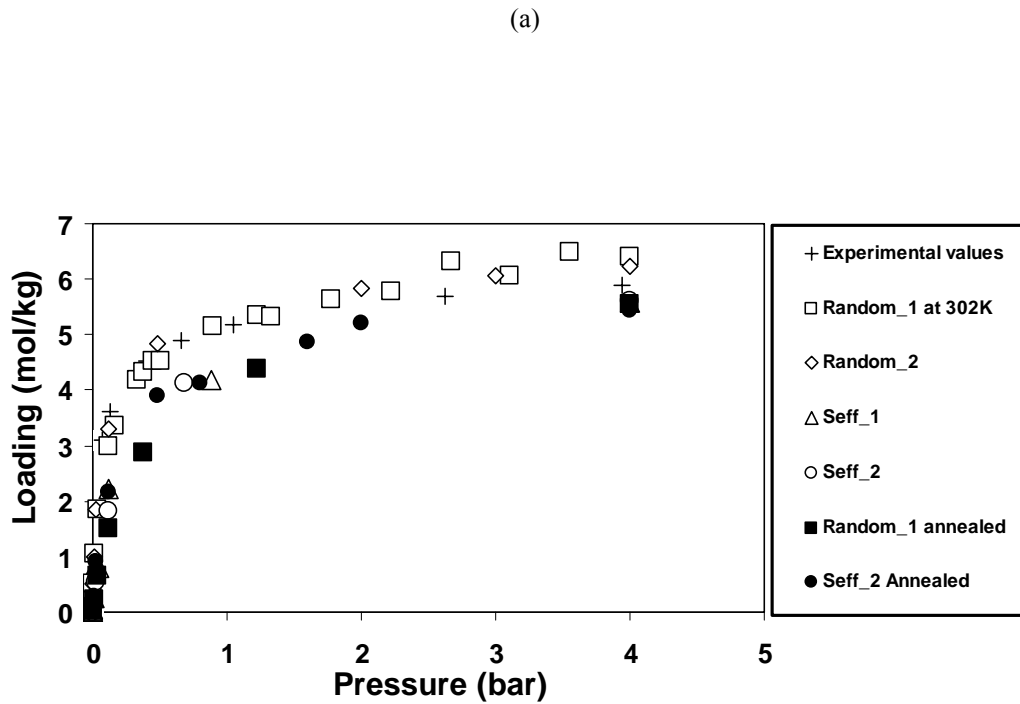


FIGURE 5. CO<sub>2</sub> adsorption isotherms in various NaX samples at (a) 302K and (b) 325K: Crosses represent experimental observations. Open and filled symbols correspond to non-annealed and annealed structures, respectively.

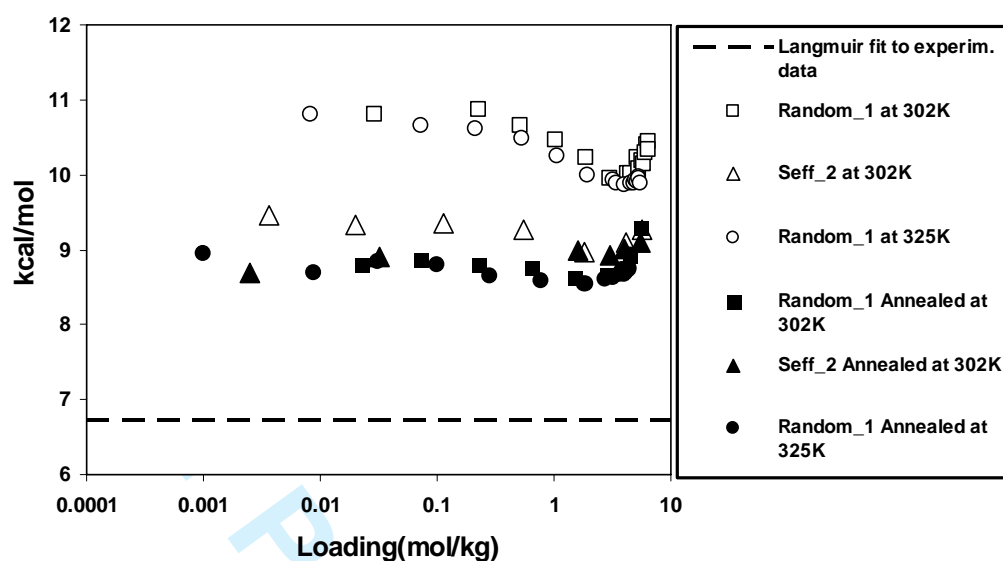


FIGURE 6. Heat of CO<sub>2</sub> adsorption. Initial NaX (non-annealed) structure for 302K and 325K. Open and filled symbols correspond to non-annealed and annealed structures, respectively.

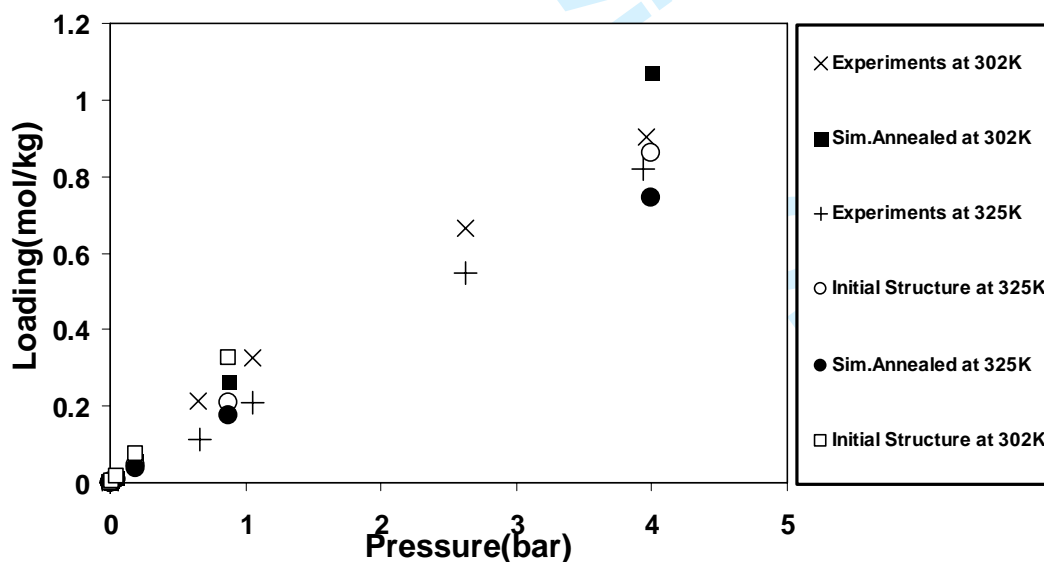


FIGURE 7. N<sub>2</sub> adsorption isotherms at 302K and 325K. Experimental observations [+] and [×] at 302 and 325 K, respectively. Open and filled symbols correspond to non-annealed and annealed structures, respectively.

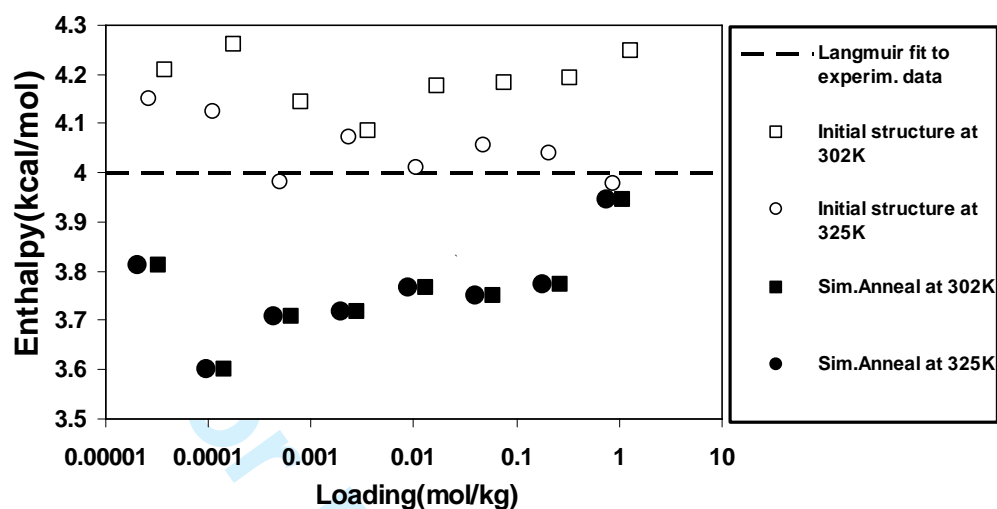


FIGURE 8. Heat of  $N_2$  adsorption. Open and filled symbols correspond to non-annealed and annealed structures, respectively.

## Conclusions

The atomistic reconstruction of NaX FAU crystals that was accomplished in this work revealed several interesting issues that have to be addressed in the study of adsorption in aluminosilicate zeolites. The positions of the framework atoms and of the non-framework cations have been determined at different temperatures using simulated annealing and their effect on  $CO_2$  and  $N_2$  sorption has been studied. More specifically, monitoring of tagged  $Na^+$  during various annealing cycles showed that the positions close to the framework Si atoms are not favorable for  $Na^+$ , which relocate themselves to positions close to Al atoms. The present work makes a clear distinction among the three particular positions in the FAU cell belonging to the site III family, as dictated by recent findings, whereas simpler models in the literature only predict up to two site III variations.

Adsorption isotherms were simulated and compared to experimental data for the same conditions. It was found that the use of non-annealed and annealed structures leads to satisfactory or even excellent agreement with experiments, depending on the degree of annealing. In any case, the deviation is smaller than the deviation between different sets of experiments for the same system under the same conditions, as reported in the

1  
2  
3  
4  
5 literature. The main benefit from the simulated annealing is that the statistical  
6 deviation in the energy calculations is reduced by almost two orders of magnitude  
7 compared to that in calculations that employed the non-annealed structure. Similar  
8 conclusions can be drawn with respect to the calculated heat of adsorption for CO<sub>2</sub>  
9 and N<sub>2</sub> in the same structures. The calculated heats of adsorption were very close to  
10 the experimental ones. It was also interesting to note a satisfactory agreement between  
11 the heats of adsorption for annealed and non-annealed structures.  
12  
13  
14  
15  
16

17  
18 In addition to Monte Carlo simulation of the adsorption isotherms, molecular  
19 dynamics can be used as well with the additional advantage that they can reveal  
20 accessibility effects on the loading calculation at different pressure levels, which are  
21 possibly overlooked in the standard sorption simulation. This is the subject of current  
22 work by the authors.  
23  
24  
25  
26

### 27 28 Acknowledgements

29  
30 The authors acknowledge EU NoE NanoMemPro for financial support. We also thank  
31 Prof. M. Tsapatsis from University of Minnesota for providing access to the magnetic  
32 microbalance facility and Dr. I.G. Giannakopoulos for running the adsorption  
33 measurements.  
34  
35  
36  
37

### 38 39 References

- 40  
41  
42  
43 [1] Krishna, R. and Van Baten, J.M. (2007) "Using molecular simulations for  
44 screening of zeolites for separation of CO<sub>2</sub>/CH<sub>4</sub> mixtures", *Chem. Eng. J.* **133**,  
45 121.  
46  
47 [2] Jia, W. and Murad, S. (2005) "Separation of gas mixtures using a range of zeolite  
48 membranes: A molecular-dynamics study", *J. Chem. Phys.* **122**, 234708.  
49  
50 [3] Krishna, R., Baur, R. (2003) "Modelling issues in zeolite based separation  
51 processes", *Sep. Purif. Technol.* **33** 213.  
52  
53 [4] Langmi, H.W., Book, D., Walton, A., Johnson, S.R., Al-Mamouri, M.M.,  
54 Speight, J.D., Edwards, P.P., Harris, I.R. and Anderson, P.A. (2005) "Hydrogen  
55 storage in ion-exchanged zeolites", *Journal of Alloys and Compounds* **404**, 637.  
56  
57 [5] Walton, K.S., Abney, M.B. and LeVan, M.D. (2006) "CO<sub>2</sub> adsorption in Y and X  
58 zeolites modified by alkali metal cation exchange", *Micropor. Mesopor. Mater.*  
59 **91**, 78.  
60



- 1  
2  
3  
4  
5  
6  
7 [6] Maurin, G., Llewellyn, Ph., Poyet, Th. and Kuchta, B. (2005) "Influence of  
8 Extra-Framework Cations on the Adsorption Properties of X-Faujasite Systems:  
9 Microcalorimetry and Molecular Simulations", *J. Phys. Chem. B*, **109**, 125.
- 10  
11 [7] Fuchs, A.H. and. Cheetham, A. K. (2001) "Adsorption of Guest Molecules in  
12 Zeolitic Materials: Computational Aspects", *J. Phys. Chem. B*, **105** (31), 7375.
- 13  
14 [8] Yashonath, S., Demontis, P. and Klein, M.L. (1991) "Temperature and  
15 Concentration Dependence of Adsorption Properties of Methane in NaY: A  
16 Molecular Dynamics Study", *J. Phys. Chem.*, **95**, 5881.
- 17  
18 [9] Suzuki, S., Takaba, H., Yamaguchi, T. and Nakao, S. (2000) "Estimation of gas  
19 permeability of a zeolite membrane, based on a molecular simulation technique  
20 and permeation model", *J. Phys. Chem. B* **104**, 1971.
- 21  
22 [10] Bakker, W.J.W., Kapteijn, F., Poppe, J., Moulijn, J.A. (1996) "Permeation  
23 characteristics of a metal-supported silicalite-1 zeolite membrane", *J. Mem. Sci.*  
24 **117**, 57.
- 25  
26 [11] Mohanty, S. and McCormick, A.V. (1999) "Prospects for principles of size and  
27 shape selective separations using zeolites", *Chem. Eng. J.* **74**, 1.
- 28  
29 [12] Guliants, V.V., Mullhaupt, J.T., Newsam, J.M., Gorman, A.M., and Freeman,  
30 C.M. (1999) "Predicting locations of non-framework species in zeolite materials",  
31 *Catal. Today* **50**, 661.
- 32  
33 [13] Verweij, H. (2003) "Ceramic membranes: Morphology and transport", *J. Mater.*  
34 *Sci.* **38**, 4677.
- 35  
36 [14] Murad, S., Jia, W. and Krishnamurthy, M. (2003) "Molecular simulations of ion  
37 exchange in NaA zeolite membranes", *Chem. Phys. Lett.* **369**, 402.
- 38  
39 [15] Jia, W. and Murad, S. (2004) "Molecular dynamics simulations of gas separations  
40 using faujasite-type zeolite membranes", *J. Chem. Phys.* **120**, 4877.
- 41  
42 [16] Navascués, N., Skouras, E.D., Nikolakis, V., Burganos, V., V.N., Tellez, C. and  
43 Coronas, J. (2007) "Reconstruction of umbite framework variants by atomistic  
44 simulations using XRD and sorption data", *Chem. Eng. Process.*, in print.
- 45  
46 [17] Navascués, N., Skouras, E.D., Nikolakis, V., Burganos, V., V.N., Tellez, C. and  
47 Coronas, J. and Santamaria, J. (2006) "Exploring chemical composition effects  
48 on umbite structure and gas separation properties using atomistic simulations",  
49 *Desalination* **199**, 368.
- 50  
51 [18] Rappé, A. K., Casewit, C. J., Colwell, K.S., Goddard III, W. A. and Skiff, W. M.  
52 (1992) "UFF, a full periodic-table force-field for molecular mechanics and  
53 molecular-dynamics simulations", *J. Am. Chem. Soc.* **114**, 10024.
- 54  
55 [19] Mayo, S.L., Olafson B.D. and. Goddard, W.A. (1990) "DREIDING: a generic  
56 force field for molecular simulations", *J. Phys. Chem.* **94**, 8897.
- 57  
58 [20] Ramsahye, N.A. and Bell, R.G. (2005) "Cation Mobility and the Sorption of  
59 Chloroform in Zeolite NaY: Molecular Dynamics Study", *J. Phys. Chem B* **109**,  
60 4738.

- 1  
2  
3  
4  
5  
6  
7 [21] Skouras, E.D., Burganos, V. and Payatakes A.C. (1999) "Simulation of gas  
8 diffusion and sorption in nanoceramic semiconductors", *J. Chem. Phys.* **110**,  
9 9244.
- 10 [22] Skouras, E.D., Burganos, V. and Payatakes A.C. (2001) "Improved atomistic  
11 simulation of diffusion and sorption in metal oxides", *J. Chem. Phys.* **114**, 545.
- 12 [23] Kusakabe, K., Kuroda, T., Murata, A. and Morooka, S. (1997) "Formation of a  
13 Y-Type membrane on a porous -alumina tube for gas separation" *Ind. Eng.*  
14 *Chem. Res.* **36**, 649.
- 15 [24] Gu, X., Dong, J. and Nenoff T.M. (2005) "Synthesis of Defect-Free FAU-Type  
16 Zeolite Membranes and Separation for Dry and Moist CO<sub>2</sub>/N<sub>2</sub> Mixtures" *Ind.*  
17 *Eng. Chem. Res.*, **44** (4), 937.
- 18 [25] Zhu L. and Seff, K. (1999) "Reinvestigation of the Crystal Structure of  
19 Dehydrated Sodium Zeolite X" *J. Phys. Chem. B* **103**, 9512.
- 20 [26] Buttefey, S., Boutin, A., Mellot-Draznieks, C. and Fuchs, A.H. (2001) "A Simple  
21 Model for Predicting the Na<sup>+</sup> Distribution in Anhydrous NaY and NaX Zeolites",  
22 *J. Phys. Chem. B*, **105**, 9569.
- 23 [27] Jaramillo, E. and Auerbach, M. (1999) "New Forcefield for Na Cations in  
24 Faujasite-Type Zeolites" , *J. Phys. Chem. B* **103**, 9589.
- 25 [28] Löwenstein, W. (1954) "The Distribution of Aluminum in the Tetrahedra of  
26 Silicates and Aluminates", *Am. Mineral.*, **39**, 92
- 27 [29] Krokidas, P., Skouras, E.D., Nikolakis, V. and Burganos, V.N. (2007) "Molecular  
28 simulation of sorption and separation in hydrated and non hydrated zeolites",  
29 *Proc. 3<sup>rd</sup> Panhellenic Symp. Porous Mater.*
- 30 [30] Krokidas, P., Skouras, E.D., Nikolakis, V. and Burganos, V.N. (2007)  
31 "Investigation of gas sorption and separation in zeolites using molecular  
32 simulation techniques", *4<sup>th</sup> Int. Zeolite Membr. Meeting, Zaragoza, Spain.*
- 33 [31] Plant, D.F., Maurin, G., Jobic, H. and Llewellyn, P. L. (2005) "Molecular  
34 Dynamics Simulation of the Cation Motion upon Adsorption of CO<sub>2</sub> in Faujasite  
35 Zeolite Systems ", *J. Phys. Chem B* **110** (29), 14372.
- 36 [32] Murthy, C. S., Singer, K., Klein, M. L. and McDonald, I. R. (1980) "Pairwise  
37 additive potential for nitrogen", *Mol. Phys.*, **41** (6), 1387.
- 38 [33] Akten, E.D., Siriwardane, R. and Sholl, D.S. (2003) "Monte Carlo Simulation of  
39 Single- and Binary-Component Adsorption of CO<sub>2</sub>, N<sub>2</sub>, and H<sub>2</sub> in Zeolite Na-4A  
40 ", *Energ Fuel* **17** (4),
- 41 [34] Maurin, G., Bell, R. G., Devautour, S., Henn, F. and Giuntini, J., C. (2004)  
42 "Modelling the effect of Hydration in Zeolite Na<sup>+</sup> - Mordenite", *J. Phys. Chem B*,  
43 **108**, 3739.
- 44 [35] Giddy, A.P., Dove, M.T., Pawley, G.S. and Heine, V. (1993) "The determination  
45 of rigid-unit modes as potential soft modes for displacive phase transitions in  
46 framework crystal structures", *Acta Cryst.*, **A49**, 697.
- 47  
48  
49  
50  
51  
52  
53  
54  
55  
56  
57  
58  
59  
60

- 1  
2  
3  
4  
5  
6  
7 [36] Smith, J.M. and Van Ness, H.C. (1987) "Introduction to chemical engineering  
8 thermodynamics", McGraw-Hill Chemical Engineering Series.
- 9  
10 [37] Frenkel, D. and Smit, B. (2002) " Understanding Molecular Simulation: From  
11 algorithms to applications", Academic Press.
- 12  
13 [38] Deem, M.W. and Newsam, J.M. (1992) "Framework Crystal Structure Solution  
14 by Simulated Annealing: Test Application to Known Zeolite Structures", *J. Am.*  
15 *Chem. Soc.*, **114**, 7189
- 16  
17 [39] Olson, D. H. (1995) "The crystal structure of dehydrated NaX", *Zeolites*, **15**,  
18 439.
- 19  
20 [40] Qiu, S., Yu, J., Zhu, G., Terasaki, O., Nozue, Y., Pang, W. and Xu, R. (1998)  
21 "Strategies for the synthesis of large zeolite single crystals", *Microporous*  
22 *Mesoporous Mater.*, **21**, 245.
- 23  
24 [41] Nikolakis, V., Xomeritakis, G., Abibi, A., Dickson, M., Tsapatsis, M. and  
25 Vlachos, D.G. (2001) "Growth of a faujasite-type zeolite membrane and its  
26 application in the separation of saturated/unsaturated hydrocarbon mixtures", *J.*  
27 *Membr. Sci.* **184**(2), 209.
- 28  
29 [42] Giannakopoulos, I.G., Kalabaliki, K., Drakopoulos, V. and Nikolakis, V. (2005)  
30 "Synthesis of faujasite membranes for the separation of propane/propylene  
31 mixtures", *Stud. Surf. Sci. Catal.* **158**(1), 137
- 32  
33 [43] Baimpos, T., Giannakopoulos, I. G., Nikolakis, V. and Kouzoudis, D. (2008)  
34 "Effect of Gas Adsorption on the Elastic Properties of Faujasite Films Measured  
35 Using Magnetoelastic Sensors" *Chem. Mater.*, **20**, 1470.
- 36  
37 [44] Lee, J.S., Kim, J.H., Kim, J.T., Suh, J.K., Lee, J.M. and Lee, C.H. (2002)  
38 "Adsorption Equilibria of CO<sub>2</sub> on Zeolite 13X and Zeolite X/Activated Carbon  
39 Composite", *J. Chem. Eng. Data*, **47**, 1237
- 40  
41 [45] Dunne, J.A., Rao, M., Sircar, S., Gorte, R.J. and Myers, A.L. (1996)  
42 "Calorimetric Heats of Adsorption and Adsorption Isotherms. 2. O<sub>2</sub>, N<sub>2</sub>, Ar, CO<sub>2</sub>,  
43 CH<sub>4</sub>, C<sub>2</sub>H<sub>6</sub>, and SF<sub>6</sub> on NaX, H-ZSM-5, and Na-ZSM-5 Zeolites", *Langmuir*, **12**,  
44 5896
- 45  
46 [46] Cavenati, S., Grande, C.A. and Rodrigues, A.E. (2004) "Adsorption Equilibrium  
47 of Methane, Carbon Dioxide, and Nitrogen on Zeolite 13X at High Pressures", *J.*  
48 *Chem. Eng. Data*, **49**, 1095.
- 49  
50  
51  
52  
53  
54  
55  
56  
57  
58  
59  
60